Wide temperature range operation of micrometer-scale silicon electro-optic modulators

Sasikanth Manipatruni, Rajeev K. Dokania, Bradley Schmidt, Nicolás Sherwood-Droz, Carl B. Poitras, Alyssa B. Apsel, and Michal Lipson*

School of Electrical and Computer Engineering, Cornell University, Ithaca, New York 14853, USA
**Corresponding author: ml292@cornell.edu*

Received April 11, 2008; revised June 20, 2008; accepted July 15, 2008;
posted August 27, 2008 (Doc. ID 94961); published September 24, 2008

We demonstrate high bit rate electro-optic modulation in a resonant micrometer-scale silicon modulator over an ambient temperature range of 15 K. We show that low bit error rates can be achieved by varying the bias current through the device to thermally counteract the ambient temperature changes. Robustness in the presence of thermal variations can enable a wide variety of applications for dense on chip electronic photonic integration. © 2008 Optical Society of America

OCIS codes: 130.3990, 130.3120.

High-speed electro-optic modulation in silicon is a crucial requirement for integration of silicon photonics with microelectronics. High-speed gigabits per second modulators have been demonstrated recently using either resonant structures [1–3] or Mach–Zehnder interferometers [4–6]. Resonant electro-optic modulators are ideally suited for dense optical networks on chips due to their compact size, high extinction ratio (ER) per unit length, low insertion loss, and low power consumption. However, resonant electro-optic modulators suffer from temperature sensitivity owing to the relatively large thermo-optic effect in silicon [7].

In this Letter, we demonstrate that the effect of thermal variations on resonant electro-optic modulators can be locally compensated by adjusting the bias current passing through the device. The bias current through the device is varied to compensate for changes in the ambient temperature that affect the resonator. We show that low bit error rate (BER) modulation can be maintained over a temperature range of 15 K. Robustness in the presence of environmental conditions, such as thermal variation, can enable a wide variety of applications in low-cost complementary metal-oxide semiconductor (CMOS) systems.

The device we demonstrate is a silicon electro-optic ring modulator fabricated on a silicon-on-insulator (SOI) substrate. The modulator is formed by building a p-i-n junction around a ring resonator with a quality factor of ~4000 and a diameter of 10 μm. The structure of the electro-optic device is shown in Fig. 1. The transmission spectrum for quasi-TM polarized light (major electric field component perpendicular to the plane of silicon) is shown in Fig. 2(a). At a constant temperature, the optical transmission through the ring is modulated using a nonreturn-to-zero (NRZ) bit sequence at 1 Gbit/s. The refractive index of the ring is modulated by active carrier injection and extraction using the p-i-n diode junction. The modulated output waveform and eye diagram at 1 Gbit/s at a nominal temperature of operation (298 K) is shown in Fig. 2(b). An on–off extinction ratio (ER) of 5 dB is measured in accordance with the transmission characteristics with a ±4 V applied voltage. The high applied voltage is attributed to a large contact resistance of the device (1.7 $k\Omega$) that can be greatly reduced by optimizing the fabrication process [8]. The power consumption is estimated as 4.52 pJ/bit with an estimated carrier lifetime of 500 ps and an injection level of 5×10^{17} cm^{-3} and taking into account both the switching and the state holding power. The power consumption can be further reduced to ~200 fJ/bit by lowering the drive voltage [8] and the device radius.

We analyzed the effect of temperature shift on the silicon electro-optic modulator over a temperature range of 15 K. The thermo-optic coefficient (TOC) of silicon is given by $\Delta n/\Delta T = 1.86\times10^{-4}\mathrm{K}^{-1}$, which leads to a resonance shift of ~0.11 nm/K from the base resonant wavelength. The large value of TOC of silicon can be attributed to the strong temperature

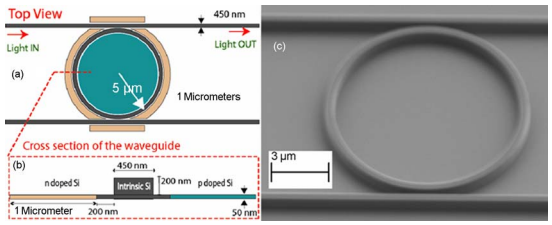

Fig. 1. (Color online) (a) Schematic of the electro-optic ring device. (b) Cross section of the waveguide embedded in a p-i-n junction. (c) Scanning electron microscope image of the ring resonator before the definition of doped regions and contacts.

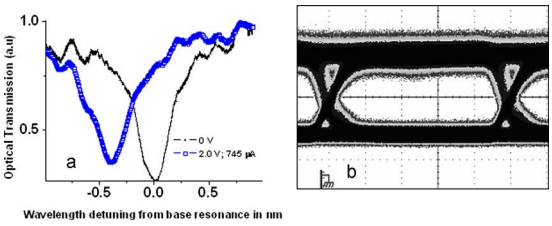

Fig. 2. (Color online) (a) Transmission spectra of the electro-optic modulator under varying dc bias voltages. (b) Eye diagram at 1 Gbit/s. All the above measurements were performed at nominal operating temperature ($\Delta T = 0$ K).

0146-9592/08/192185-3/$15.00

dependence of the bandgaps of silicon [9]. Figure 3(a) shows the spectral shift as the temperature of the chip is varied over 4 K. Figure 3(b) shows the distorted eye diagrams under a 2 K temperature shift. We also compare the effect of thermal shift on the modulated waveforms with electro-optic simulations and show a good match between simulation and experiment as shown in Fig. 4(a). A description of the electro-optic modeling is presented elsewhere [10]. The simulated and measured waveforms with a 15 K shift in temperature are shown in Fig. 4(b).

To enable a wide temperature operation of resonant silicon electro-optic modulators, we propose and implement local thermal control of the waveguide temperature by changing the bias current through the device. Using a dc bias current we first set the nominal operating condition of the modulator, and as the ambient temperature varies we vary the dc bias current to maintain the local temperature of the device at the original value. As we vary the bias current of the p-i-n junction, the heat generated in the waveguides allows control over the local temperature of the waveguide forming the resonator.

Using this control technique, we experimentally demonstrate a wide temperature range, 15 K, operation of the resonant silicon electro-optic modulator. To control the dc bias current through the device, we add the high-speed rf signal to a dc current source using a bias tee. A capacitor of 20 nF avoids the loading of the bit pattern generator by the dc bias supply, and an inductor of 1 mH isolates the dc source from the bit pattern. The dc bias current is varied to counter the effect of the temperature change for retrieving the bit pattern. The base operating condition was set with a 1.36 mA dc current through the device with a 0.2 V bias voltage. The current was reduced to 345 μA (with a 2.2 V bias voltage) to maintain the modulation when the ambient temperature was raised by 15 K. Note that the current measured is the time averaged extraction current during the reverse bias of the device. Note that even though the bias current produces an index change due to the injected carriers in the on state, the effect of carrier dispersion due to the bias current is absent in the off state. Hence, the bias current is contributing only in regulating the temperature of the waveguides. The temperature of the heat sink is controlled through an external temperature controller with feedback. The joule thermal power consumption for maintaining the base operating condition is estimated as

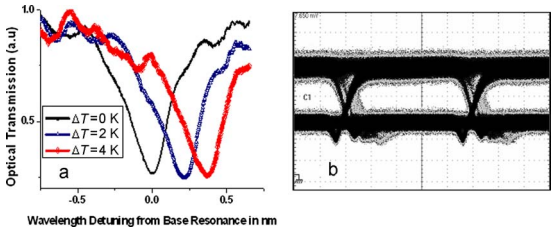

Fig. 3. (Color online) (a) Transmission spectra with varying ambient temperature with no current through the device. (b) Distorted eye diagram at $\Delta T=2$ K, 1 Gbit/s. Applied ac-modulated voltage and wavelength of operation were unchanged.

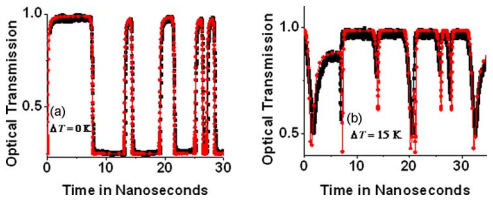

Fig. 4. (Color online) Simulation of the waveform distortion due to thermal effects. (a) Baseline simulations at $\Delta T=0$ K. (b) Distorted waveforms at $\Delta T=15$ K; gray curves show the electro-optic device computer simulations, and the black curves show the measured waveforms.

3.1 pJ/bit at $\Delta T=0$ K and 200 fJ/bit at $\Delta T=15$ K. Both of these values can be further reduced significantly by device optimization.

We show open eye diagrams with a clear eye opening over 15 K by controlling the dc bias current to maintain the local temperature of the ring at the original operating condition as shown in Fig. 5. We kept the operating wavelength constant at 1553.98 nm. We estimate the quality factor of the eye diagrams $Q=|\mu_2-\mu_1|/(\sigma_2+\sigma_1)$ to be 11.35 at the nominal operating temperature. The retrieved quality factor at $\Delta T=15$ K is 7.15. These Q values are sufficient for a BER of 10^{-12} [11]. The rise and fall times are ~300 ps. A 2^9-1 NRZ pseudorandom bit sequence (PRBS) was used for these experiments. The predicted thermal time constants (T_c) are of the order of microseconds. Hence the effect of the length of the longest sequence of ones or zeros will be significant for PRBS signals with more than (T_c/bit period) consecutive ones or zeros. For example, at 1 Gbit/s with a T_c of 1 μs the PRBS length is limited to hundreds of consecutive bits. Similar run length limitations are common in digital encoding schemes, such as $8b/10b$ [12]. Note that this limitation becomes less stringent as the bit rate is increased.

We compare the power efficiency of the proposed local temperature control method with the commonly used metal strip heater method. We use two-dimensional heat flow, which takes into consideration conduction of heat to the substrate and the radiative heat loss through the top surface of the chip. The thermal modeling was carried out in a multiphysics finite-element simulator. The loss through the top surface is modeled via the Stefan–Boltzman law with emissivity factors of 0.94 for SiO_2 and 0.33 for the smooth metal layer. We assumed that the bottom of the wafer as the heat sink was maintained at 300 K

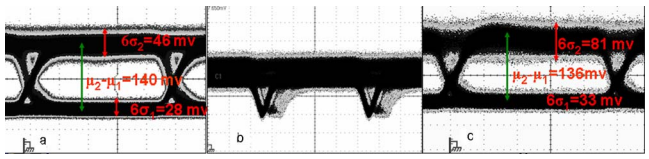

Fig. 5. (Color online) Optical transmission eye diagrams at various thermal and bias current conditions. Eye diagrams (a) at $\Delta T=0$ K, 1.36 mA, (b) degraded at $\Delta T=15$ K, 1.36 mA, and (c) retrieved at $\Delta T=15$ K, 345 μA. PRBS 2^9-1 bit sequences were used for all measurements. Applied ac-modulated voltage and wavelength of operation were kept constant.

(T_{amb}). We also assumed a 3 μm buried oxide layer and 1 μm top cladding oxide. The top cladding layer is chosen to be 1 μm so that the heating due to the metal layers is optimal while limiting the optical losses due to mode overlap with metal [13]. We assumed a heat source of 1 mW/μm^3 localized within the metal layer or the waveguide to compare the efficiency. We also assumed that the metal heaters were perfectly aligned with the waveguides for optimal heating. The simulations show that the temperature difference produced by direct localized heating using the p-i-n structure is significantly larger than the metal strip heater method (see Fig. 6). We compared the temperature difference ($\Delta T = T_{local} - T_{amb}$) at the center of the waveguide produced by both methods. The direct localized heating using a p-i-n structure produces $\Delta T = 40.1$ K/(mW/μm^3) [Fig. 6(b)], while a metal heater positioned on top produces $\Delta T = 21.3$ K/(mW/μm^3) [Fig. 6(a)]. Hence, the simulations show that the direct localized heating method is approximately twice as efficient as the metal heater. An added advantage of using the direct localized heating method technique is that it requires fewer fabrication steps as it makes use of the existing structure (i.e., the contacts of the p-i-n device) to achieve thermal tuning. The use of CMOS compatible low power consumption temperature sensors is a common practice in the microprocessor industry [14]. Using efficient sensors the energy for sensing can be as small as 10 fJ/bit. Moreover, since the time response of thermal effects is relatively slow ($T_c \approx 1$ μs), a relatively crude temperature sensor can be integrated for achieving a wide temperature operation of resonantly enhanced modulators.

In summary, we have shown a wide temperature range operation of resonant micrometer scale modulators while ensuring high-speed operation. We demonstrated low bit error rate waveforms over a 15 K range while maintaining a bit rate of 1 Gbit/s. In light of the recent demonstration of high speed, low insertion loss, and small footprint (18 Gbits/s, <1 dB, 10 μm) modulators [15], the wide temperature range operation of resonant compact electro-optic modulators has significant impact for the large scale integration of compact modulators for dense on chip optical networks.

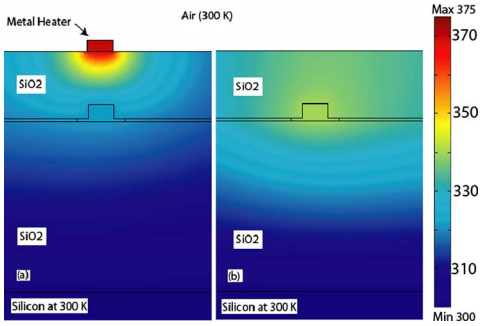

Fig. 6. (Color online) Temperature profiles using (a) metal strip heater and (b) direct localized waveguide heating. The gradient bar indicates the temperature scale in Kelvin.

This work was sponsored by the Defense Advanced Research Projects Agency (DARPA) supervised by Jagdeep Shah and executed by the U.S. Army Research Office (ARO) under contract W911NF-06-1-0057 managed by Wayne Chang. This work was also supported by the National Science Foundation (NSF) CAREER grants 0446571 and 0347649, Applied Research Laboratories (ARL) contract W911NF-07-1-0652 managed by Sankar Basu. This work was performed in part at the Cornell NanoScale Facility, a member of the National Nanotechnology Infrastructure Network, which is supported by the NSF grant ECS-0335765.

References

1. Q. Xu, B. Schmidt, S. Pradhan, and M. Lipson, Nature **435**, 325 (2005).
2. B. Schmidt, Q. Xu, J. Shakya, S. Manipatruni, and M. Lipson, Opt. Express **15**, 3140 (2007).
3. L. Zhou and A. W. Poon, Opt. Express **14**, 6851 (2006).
4. A. Liu, R. Jones, L. Liao, D. Samara-Rubio, D. Rubin, O. Cohen, R. Nicolaescu, and M. Paniccia, Nature **427**, 615 (2004).
5. S. J. Spector, M. W. Geis, G.-R. Zhou, M. E. Grein, F. Gan, M. A. Popovic, J. U. Yoon, D. M. Lennon, E. P. Ippen, F. Z. Kärtner, and T. M. Lyszczarz, Opt. Express **16**, 11027 (2008).
6. W. M. Green, M. J. Rooks, L. Sekaric, and Y. A. Vlasov, Opt. Express **15**, 17106 (2007).
7. M. Lipson, IEEE J. Sel. Top. Quantum Electron. **12**, 1520 (2006).
8. W. L. Yang, T. F. Lei, and C. L. Lee, Solid-State Electron. **32**, 997 (1989).
9. Y. P. Varshni, Physica (Amsterdam) **34**, 149 (1967).
10. S. Manipatruni, Q. Xu, and M. Lipson, Opt. Express **15**, 13035 (2007).
11. I. Shake, H. Tikara, and S. Kawanishi, J. Lightwave Technol. **22**, 1296 (2004).
12. A. X. Widmer, and P. A. Franaszek, IBM J. Res. Dev. **27**, 440 (1983).
13. F. Gan, T. Barwicz, M. A. Popovic, M. S. Dahlem, C. W. Holzwarth, P. T. Rakich, H. I. Smith, E. P. Ippen, and F. X. Kartner, in *Proceedings of the IEEE/LEOS Photonics in Switching* (IEEE, 2007), pp. 67–68.
14. A. Naveh, E. Rotem, A. Mendelson, S. Gochman, R. Chabukswar, K. Krishnan, and A. Kumar, Intel Technol. J. **10**, 109 (2007).
15. S. Manipatruni, Q. Xu, B. Schmidt, J. Shakya, and M. Lipson, in *Proceedings of the Lasers and Electro-Optics Society (LEOS 2007)* (IEEE, 2007), p. 537.